Prediction of Cracking in Soil-Cement

by
R. J. DUNLOP, B.E., Ph.D.
Engineer, Ministry of Works and Development, N.Z.
P. J. MOSS, B.E.(Hons), Ph.D., D.I.C.
Senior Lecturer, Department of Civil Engineering, University of Canterbury, N.Z.
and
T. A. H. DODD, B.E.(Hons)
Senior Lecturer, Department of Civil Engineering, University of Canterbury, N.Z.

SUMMARY

This paper discusses the effect of internal stresses on the cracking of a soil cement base and reviews previous work on the subject. Research undertaken at the University of Canterbury to investigate the mechanisms involved in the cracking of a soil-cement pavement is summarised and discussed.

This research places particular emphasis on the development of the shrinkage stresses in a soil-cement base. Because existing methods for predicting shrinkage stresses were found to be inadequate, a new method of stress prediction based on a combination of experimental results and fundamental theory is presented. The phenomenon of "stress reversal" within a drying soil cement prism is also discussed.

Conclusions from the research are that the method of stress determination outlined in the paper can be used to predict shrinkage stresses, providing the moisture distribution within the soil-cement base is known.

1.0 INTRODUCTION

Cracking of road pavements is not only unsightly but also affects the riding quality of the road and permits the ingress of water to the subgrade. For a soil-cement base, cracking is caused mainly by shrinkage stresses, temperature stresses, traffic loading and subgrade failure. Of these four factors, the first three could be taken into account when designing the pavement. However, to date, little comprehensive research into shrinkage stresses has been carried out, although a better understanding of the mechanics of crack formation in soil-cement pavements could enable designers to allow for cracking, or even to eliminate it altogether.

Shrinkage within soil-cement occurs during moisture loss, either by self-desiccation (i.e. loss of moisture from the soil matrix to the hydrating cement) or by drying (i.e. loss of moisture to the atmosphere). Of these two, the drying shrinkage is by far the most important and consequently most of the research discussed in this paper considers the behaviour of soil-cement while drying.

Several papers dealing with cracking in soil-cement bases have been reviewed in a thesis by the first Author (1) where it was noted that much of the previous research either over-simplified the problems, or used complex theoretical analyses but ignored a number of the fundamental factors that are involved. Of this previous research, the work carried out by Okada and Kawamura (2) showed the most promise, though their theoretically predicted shrinkage stresses were not compared with any experimentally determined stresses and their work was incomplete to this extent. Since the research reported in (1) was completed, several further papers on soil-cement have been published. Morling (3) considers a number of practical methods for minimising cracking while George (4) studies the development of microcracks in the vicinity of preexisting flaws in the soil-cement base. Other papers (5) (6) and (7) consider different aspects of soil-cement behaviour.

This paper outlines research carried out at the University of Canterbury to investigate the mechanisms involved when a soil-cement pavement cracks under the action of shrinkage stresses. A theoretical analysis based on the work of Okada and Kawamura (2) was applied to two New Zealand soil-cement mixes (one using a sandy pumice and the other a loess), and the stress build-up characteristics so obtained compared well with experimentally obtained results.

2.0 PROPOSED METHOD OF SHRINKAGE STRESS PREDICTION

Soil-cement prisms were subjected to the following three types of restraint during drying:

(i) Fully restrained (a 76 mm square, 286 mm long prism sealed with wax on all but two opposite drying faces, and anchored at both ends through swivel joints to a rigid frame.)

(ii) Restrained against bending (a 76 mm square, 286 mm long prism, sealed with wax on all but two opposite drying faces, but not anchored at the ends.)

(iii) Completely unrestrained (a 286 mm long prism 76 mm deep and 38 mm wide, sealed with wax on all but one 286 x 76 mm drying face, and not anchored at the ends.)

If the free unrestrained shrinkage strain S (defined as the unit linear deformation that would occur if each infinitesmal element were unrestrained) is known for any prism at any particular time, it should be possible to determine the stresses in that prism. Unless the strains resulting from the free unrestrained shrinkage happen to coincide with those necessary for continuity, additional stresses and corresponding strains will be produced, and will modify the shrinkage strains. The resultant unit deformation ε_x is defined as the algebraic sum of the free unrestrained shrinkage strain S and the strain ε_s produced by the continuity stresses. In other words, ε_x is the deformation measured as the soil-cement prism shrinks.

Dunlop has shown (1) that the strain ε_s produced by the continuity stresses for the three types of restraint mentioned above are:

(i) Fully restrained

$$\varepsilon_s = S(t) \text{ at any time } t \qquad \ldots 1$$

(ii) Restrained against deflection

$$\varepsilon_s = S(t) - S_{av}(t) \text{ at any time } t \qquad \ldots 2$$

(iii) Completely unrestrained

$$\varepsilon_s = S(t) - S_{av}(t) + \frac{(y-y_c)}{I_T}\left[\int_{-y_c}^{b-y_c} nS(t)y\,dy - \frac{b}{2}\int_{-y_c}^{b-y} S(t)\,dy\right] \ldots 3$$

at at time t .

where b = width of prism
y = coordinate across width of prism from sealed face
y_c = b - the distance from the drying face to the neutral axis
$S_{av}(t)$ = average measured shrinkage of a drying soil-cement prism at time t
n = ratio of elastic modulus at a point to that at the sealed surface
I_T = transformed moment of inertia

But when any stress is imposed on a soil-cement element, creep begins to act to relieve this stress. The creep may be represented mathematically by the Maxwell model, shown in Fig. 1.

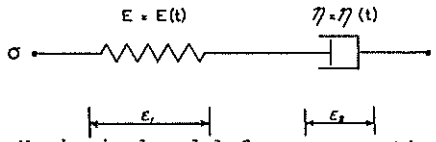

Fig. 1 Mechanical model for representing creep in a soil-cement.

In order to obtain the stress at any time t, within a fully-restrained soil-cement prism, the following equations were developed:

For a fully restrained prism,

$$\varepsilon_x(t) = 0$$

And from equation (1),

$$\varepsilon_s = S(t)$$

The total strain ε_s = elastic strain ε_1 + creep strain ε_2

$$\therefore\ S(t) = \varepsilon_1 + \varepsilon_2$$

$$\dot{S} = \dot{\varepsilon}_1 + \dot{\varepsilon}_2$$

where a dot denotes time-rate of change of the quantity.

From Fig. 1, $\sigma = E(t)\varepsilon_1 = \eta(t)\dot{\varepsilon}_2 = \eta(t)\ (\dot{S} - \dot{\varepsilon}_1)$

where $E(t)$ = modulus of elasticity at time t

and $\eta(t)$ = viscoelastic coefficient of the Maxwell model at time t

$$\therefore\ \dot{\varepsilon}_1 - \dot{S} = -\frac{E(t)}{\eta(t)}\varepsilon_1$$

$$\text{or } \dot{\varepsilon}_1 = \dot{S} - \frac{E(t)}{\eta(t)}\varepsilon_1$$

$$\text{i.e. } \dot{\varepsilon}_1 = f(\varepsilon_1, t) = \dot{S}(t) - \frac{E(t)}{\eta(t)}\varepsilon_1 \qquad \ldots 4$$

Now if $\varepsilon_1 = 0$ at $t = 0$

and $\varepsilon_1^k = \varepsilon_1(k\Delta t)$

where k is some multiple of a basic time interval Δt ,

then an approximate solution of equation 4 can be obtained:

$$\frac{\varepsilon_1^{k+1} - \varepsilon_1^k}{\Delta t} = \dot{S}(k\Delta t) - \frac{E(k\Delta t)}{\eta(k\Delta t)}\varepsilon_1^k$$

$$\therefore\ \varepsilon_1^{k+1} = \varepsilon_1^k + \Delta t\ [\dot{S}^k - \frac{E^k}{\eta^k}\varepsilon_1^k]$$

where $\dot{S}^k + \frac{S^{k+1} - S^{k-1}}{2\Delta t}$

η^k is dependent on moisture content and time

E^k is dependent on moisture content

$\therefore$ at k+1 the stress in any element of soil-cement at any time is

$$\sigma^{k+1} = E^{k+1}\varepsilon_1^{k+1} \qquad \ldots 5$$

This is the basis of the finite-element approach used to predict stresses at given positions and times within a soil-cement prism during drying.

3.0 EXPERIMENTAL WORK CARRIED OUT

In order to apply equations 1 to 5, it was necessary to carry out the experimental work outlined below.

3.1 Moisture Content

Since the moisture content parameter plays a major role in the development of shrinkage stresses in soil-cement, it was decided that moisture profiles should be determined experimentally after different periods of drying for prisms restrained as for cases (i) (ii) and (iii).

To find the moisture content profiles, six prisms were made using identical techniques. At different times a section of each prism was chopped into small pieces, and the moisture content of each piece was found. The locations of the pieces in the prism being known, the moisture gradient could be determined, and from this the moisture profiles were estimated. These were compared with theoretically obtained moisture content profiles such as those shown in Fig. 2, and a close comparison was found. Typical experimental and theoretical moisture content results are shown in Fig. 3.

3.2 Shrinkage Strains

These were measured on prisms 286 mm long by 76 mm deep, and either 38 mm or 76 mm wide. For the condition of restraint against bending, a 76 mm wide prism was used, and two opposite faces were allowed to dry, while for the completely unrestrained condition a 38 mm wide prism was used, drying from one face only. In each case the drying face was vertical, and all other faces were sealed with a flexible wax to prevent evaporation. Longitudinal length measurements were made on the top face on five parallel gauge lengths spaced across the face, using a Demec gauge. Shrinkage was calculated from the changes in these lengths.

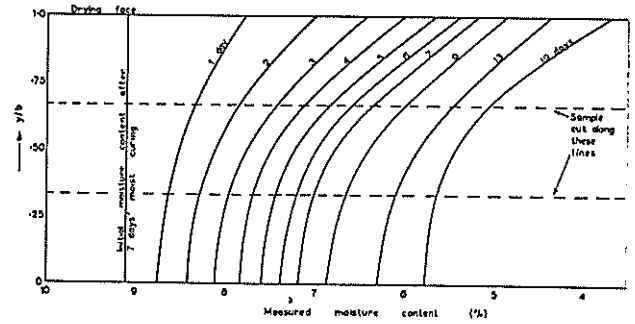

Fig. 2 Theoretical moisture content profiles for a 38 mm one side drying loess soil-cement prism.

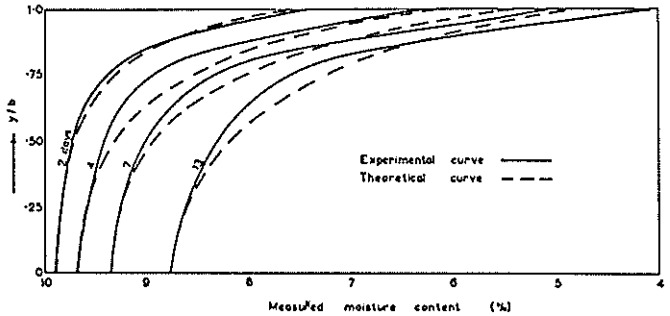

Fig. 3 Comparison of the theoretical experimental moisture content profiles for a 76 mm wide one-side drying loess soil-cement prism.

On the 38 mm wide, completely unrestrained prisms drying from one side, the phenomenon of strain reversal was first recorded. When such a prism was allowed to dry, the open face tended to dry much quicker than the remainder of the prism, so that the sample curved concave towards the drying face, but after a few days the prism would straighten and then curve concave towards the sealed face, as shown in Fig. 4 for loess soil-cement.

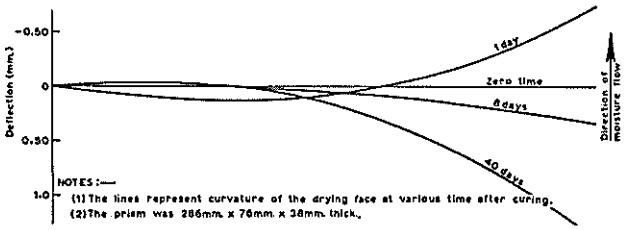

Fig. 4 Deflected shapes for a 38 mm wide loess soil-cement prism drying from one face.

Strain reversal can be explained in the following way. The elements of soil cement on the open face of a one-side-drying prism tend to shrink rapidly when drying is first initiated, but are prevented from shrinking greatly by restraint from the relatively unchanged remaining mass of the prism. This means that high tensile stresses are built up on the drying face, with consequent high strain release brought about by creep. As drying proceeds towards the sealed face, the internal soil-cement elements shrink in a similar way to the elements on the drying face, except that the internal stresses are much lower than those originally occurring on the drying face, so the strain release by creep for the internal soil-cement elements is quite low. But all soil-cement elements in a given prism have the same initial potential to shrink, so the elements at the sealed face may eventually exhibit more shrinkage than those on the drying face, because of their much lower strain release from creep. The net result is the occurrence of strain reversal.

3.3 Elastic Modulus

The elastic tension and compression moduli for specimens at specific moisture contents were obtained by rapidly loading the specimens and measuring their deflection. Samples 13 mm in diameter were used in the testing program; the elastic modulus in tension was obtained from samples loaded in direct tension. As the tensile stress-strain curves for the soil-cement studied at a constant moisture content were nearly linear for 90% of the loading range, the elastic modulus was taken as the secant modulus at the elastic limit. Curves of elastic modulus vs moisture content for loess soil-cement are illustrated in Fig. 5.

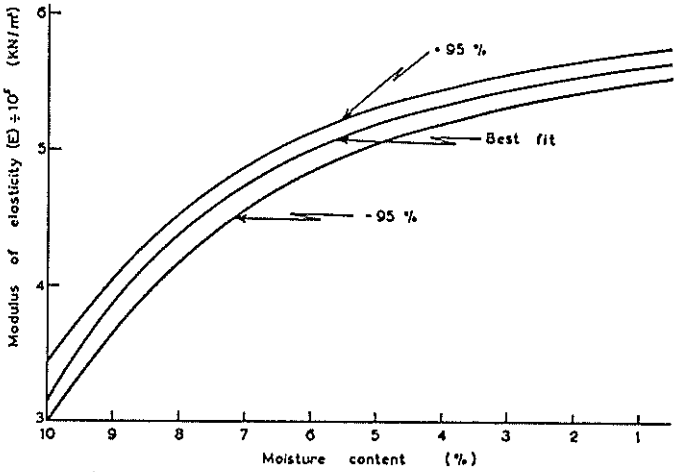

Fig. 5 Elastic modulus vs moisture content for a loess soil-cement.

3.4 Free Unrestrained Shrinkage

As explained in section 2, the free unrestrained shrinkage for a drying soil-cement has been obtained experimentally, instead of by using previously suggested theoretical methods. By drying six 13 mm diameter samples slowly, measuring at regular intervals their length and weight loss, and averaging the six results, a sufficiently reliable curve was obtained for shrinkage vs moisture content.

3.5 Creep Characteristics

A review of the literature makes it clear that more thought needs to be given to the execution of creep tests. In the past, creep has usually been measured in compression only, though in actual fact a pavement acted upon by shrinkage stresses is subject to creep in tension. Because of the non-uniform drying which develops in a large soil-cement sample, non-uniform stress build-up will result, with likely restriction of the true creep.

For this research work it was found necessary to adopt the Maxwell model to represent creep and creep release in the shrinkage stress analysis. Many other ways of representing creep were tried, but all were unsuccessful. From the many creep tests done, it was evident that both the time under stress and the moisture present in a sample influenced the viscoelastic coefficient of the Maxwell model. This led to the plotting of viscoelastic coefficients against their respective time-rates of change of moisture content for the twenty samples tested. The resulting curve, Fig. 6, was used in the

shrinkage stress analysis.

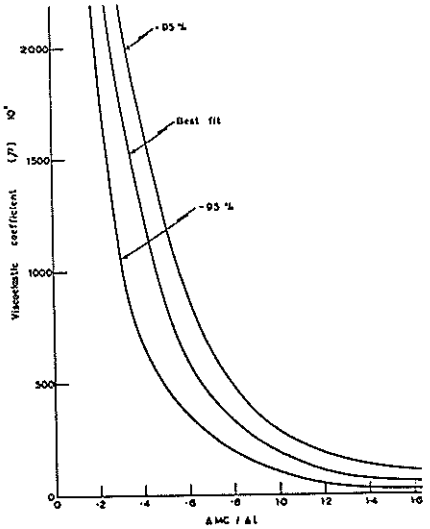

Fig. 6 Viscoelastic coefficient vs time-rate of change in moisture content for a loess soil-cement.

3.6 Tensile Strength

From the testing carried out, it was found that the ultimate tensile strength of soil-cement samples was very sensitive to moisture content at the time of the test. Consequently a tensile strength vs moisture content curve was developed from experimental results, Fig. 7, and was used in analysis for the prediction of cracking.

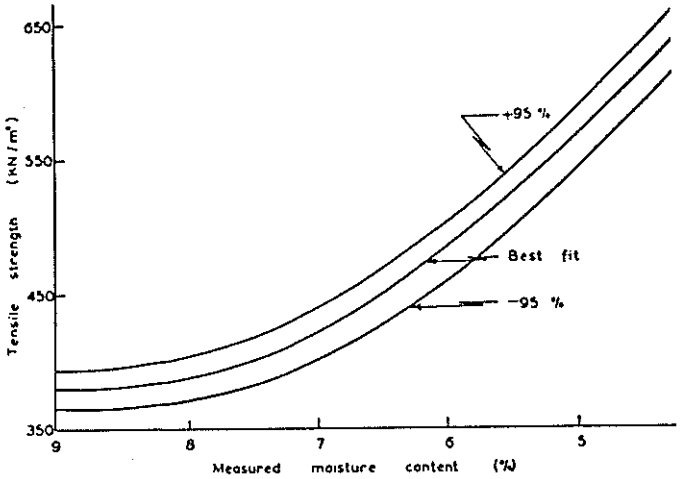

Fig. 7 Tensile strength vs moisture content for a loess soil-cement.

4.0 COMPARISON OF THE CALCULATED AND EXPERIMENTAL SHRINKAGE STRESSES

4.1 Results from Loess Soil-Cement Prisms

In order to measure the drying shrinkage strains, ε_{sx}, and the corresponding moisture content profiles, a series of samples with different widths was used. However, for the shrinkage stress analysis, the shrinkage strains used were those measured on 38 mm wide prisms drying from one face, Fig. 8. The calculated shrinkage stresses for a fully restrained 76 mm wide loess soil-cement prism are shown in Fig. 9, where these stresses are compared with the tensile strength. From this it can be seen that after six days' drying, overstress occurs internally between the centre and the sealed face of the prism. Probably the most interesting point is that the cracking caused by this overstress is initiated internally, and not on the drying face as predicted by Kawamura for concrete (8). The initial internal crack will eventually (after approximately 6½ days) propagate to an outer surface of the prism, when complete failure will occur. Experimentally, it was found that fully restrained prisms failed after 7 days' drying, so the prediction of failure time is quite good.

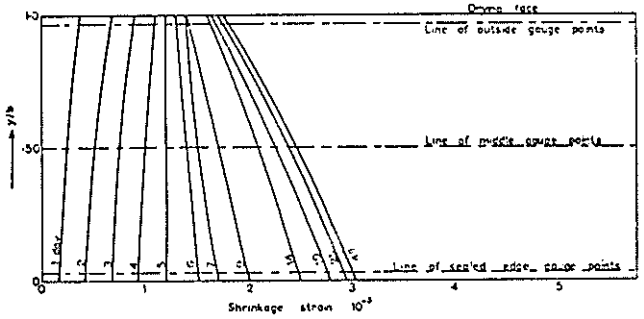

Fig. 8 Shrinkage strains for a 38 mm wide loess soil-cement prism drying from one face.

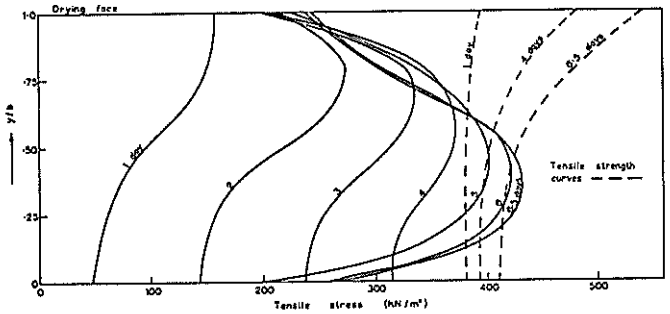

Fig. 9 Prediction of shrinkage stresses in a fully restrained 76 mm wide loess soil-cement prism drying from two sides.

For completely unrestrained loess soil-cement prisms 38 mm wide, drying from one side, the predicted curvature was found to correspond closely with the observed curvature; the strain reversal point came at 5½ days' drying time, compared with the predicted time of 5 days. The experimental deflected shape of the loess soil-cement prism, up to the time of strain reversal, corresponds very closely with the theoretical results, but past this point the two curves diverge quite markedly.

4.2 Results from Sandy Pumice Soil-Cement Prisms

For the sandy pumice soil-cement, the completely unrestrained (38 mm wide) prisms have similar characteristics to the loess soil-cement prisms of the same size, but the shrinkage stresses are much lower. Consequently it was found that failure of a fully restrained sandy pumice soil-cement prism never occurred under drying-induced shrinkage stresses.

As in the loess soil-cement prisms, strain reversal occurred also in the completely unrestrained sandy pumice soil-cement prisms, and the predicted strain reversal time was also later than the experimentally observed reversal time.

4.3 Comments

For both loess and sandy pumice soil-cement prisms, the predicted average stress build-up compared closely with the measured average stresses, though in the later stages of drying the completely unrestrained prisms of both materials deflected more than was predicted. There are several possible explanations for this discrepancy, but it is likely that the allowance made for creep in the theoretical model is the main source of error, because it was difficult to find a satisfactory representation of creep strains, by either experimental or theoretical methods. The Maxwell model adopted does not accurately simulate the deformation change which occurs in soil-cement when the load is suddenly removed, so the recoverable deformation indicated by the model is a little larger than actually occurs because of plastic yield of the soil-cement.

4.4 Summary of Discussion of the Proposed Method for Shrinkage Stress Prediction

As shown above, the shrinkage stresses which occur within soil-cement prisms can be predicted reasonably accurately, using the method outlined in section 3. The prediction proposed uses parameters evaluated from the experimental curves of free unrestrained shrinkage versus moisture content, elastic modulus versus moisture content, moisture content profiles for different periods of drying, and viscoelastic coefficients from the Maxwell model. Of the above experimental curves, the viscoelastic coefficients obtained for the soil-cement prisms cannot be taken with the same confidence as the others.

Notwithstanding the inaccuracies which still exist in the representation of creep, the proposed method for shrinkage stress prediction has provided a very reliable representation of the shrinkage behaviour of a soil-cement prism and of the shrinkage stresses which develop as it dries. It should therefore be possible to extend this method of prediction to a soil-cement pavement base, provided the moisture conditions can be predicted throughout the pavement.

The basic parameters controlling the behaviour of a soil-cement pavement base are creep, moisture flow, strength development, and shrinkage. Once these parameters are understood and evaluated, they can be inserted into the shrinkage stress equations to predict the behaviour of the pavement base. This has been done with considerable success. By combining shrinkage stresses with temperature-induced stresses and traffic loadings, crack spacing and crack widths can be predicted. This work is being prepared for publishing in a later paper.

5.0 CONCLUSIONS

The development of cracking in soil-cement prisms can be predicted, providing sufficient is known about the various properties of the particular soil-cement to enable the shrinkage stresses to be determined. However, the determination of the shrinkage stresses is complicated by the effects of moisture movement under stress, and by creep. Previously shrinkage, strength and creep have all been taken as functions of time only, but it has been found in this study that unrestrained shrinkage, strength and elastic modulus are all functions of moisture content, while creep is a function of both time and moisture content.

The method of shrinkage stress prediction proposed in this paper is based on theory, but is also utilizes experimental results that give the tensile strength, the elastic modulus, the unrestrained shrinkage, and the viscoelastic coefficients for the Maxwell model for creep, as functions of moisture content. The method, when applied to two New Zealand soil-cement mixes (one made from loess and the other from sandy pumice), gave stress build-up characteristics that compared well with experimentally obtained results.

7.0 REFERENCES

1. Dunlop, R.J., - "Shrinkage and Creep Characteristics of Soil-Cement", unpublished Ph.D. thesis, University of Canterbury, 1973.

2. Okada, K. and Kawamura, M., - "Some considerations on drying shrinkage stresses of soil-cement", Trans. of the Japan Society of Civil Engineers, (In Japanese), No. 142, pp37-45, 1967.

3. Norling, L.T., - "Minimising Reflective Cracks in Soil-Cement Pavements: A Status Report of Laboratory Studies and Field Practices", Highway Res. Rec. No. 442, pp22-33, 1973.

4. George, K.P., - "Cracking in Soil-Cement", Paper No. A76, 7th Aust. Road Res. Board Conf., Adelaide, 1974.

5. Wang, M. and Lee, K., - "Creep Behaviour of Cement-Stabilised Soils", Highway Res. Rec. No. 422, pp58-68, 1973.

6. Shackel, B. and Lee, R.H.F., - "Some Aspects of the Curing of a Soil-Cement", paper No. A21, 7th Aust. Road Res. Board Conf., Adelaide, 1974.

7. Shackel, B., - "The Behaviour of Stabilised Soils Under Simulated Traffic Loads", paper No. A22, 7th Aust. Road Res. Board Conf., Adelaide, 1974.

8. Kawamura, M., - "Shrinkage Stresses in Concrete as a Visco-elastic Material", J.A.C.I. Vol. 66, No. 12, pp968-971, Dec. 1969.